Aquatic and terrestrial takeoffs require different hindlimb kinematics and muscle function in mallard ducks

Title: Aquatic and terrestrial takeoffs require different hindlimb kinematics and muscle function in mallard ducks

Running Title: Mallard aquatic and terrestrial takeoffs

Authors: Kari R. Taylor-Burt, Andrew A. Biewener

Affiliations: Concord Field Station, Harvard University

Corresponding author email address: karitaylorburt@fas.harvard.edu

Keywords: mallard, takeoff, muscle, fascicle strain, work, kinematics

Accepted ***J. exp. Biology*** 10 June 2020

Summary Statement

Mallard ducks use environment-specific locomotor patterns (i.e., kinematics and lateral gastrocnemius muscle strain patterns) during takeoff from water versus land.

Abstract

Mallard ducks are capable of performing a wide range of behaviors including nearly vertical takeoffs from both terrestrial and aquatic habitats. The hindlimb plays a key role during takeoffs from both media. However, because force generation differs in water versus on land, hindlimb kinematics and muscle function are likely modulated between these environments. Specifically, we hypothesize that hindlimb joint motion and muscle shortening are faster during aquatic takeoffs, but greater hindlimb muscle forces are generated during terrestrial takeoffs. In this study, we examined the hindlimb kinematics and *in vivo* contractile function of the lateral gastrocnemius (LG), a major ankle extensor and knee flexor, during takeoffs from water versus land in mallard ducks. In contrast to our hypothesis, we observed no change in ankle angular velocity between media. However, the hip and metatarsophalangeal joints underwent large excursions during terrestrial takeoffs but exhibited almost no motion during aquatic takeoffs. The knee extended during terrestrial takeoffs but flexed during aquatic takeoffs. Correspondingly, LG fascicle shortening strain, shortening velocity, and pennation angle change were greater during aquatic takeoffs than terrestrial takeoffs due to the differences in knee motion. Nevertheless, we observed no significant differences in LG stress or work, but did see an increase in muscle power output during aquatic takeoffs. Because differences in the physical properties of aquatic and terrestrial media require differing hindlimb kinematics and muscle function, animals such as mallards may be challenged to tune their muscle properties for movement across differing environments.

Introduction

Navigating between terrestrial and aquatic environments presents a challenge for animals because differences in solid and fluid properties change the demands for generating propulsive forces for locomotion. As a result, movement across these media likely requires differing kinematics and muscle function (Kamel *et al.,* 1996; Biewener and

Gillis, 1999; Biewener and Corning, 2001; Gillis and Blob, 2001; Foster *et al.,* 2018). In particular, previous studies have reported differences in hindlimb kinematics and muscle function between walking and surface swimming in ducks (Biewener and Corning, 2001; Carr, 2008; Provini *et al.,* 2012A).

Mallards, *Anas platyrhynchos* (Linnaeus, 1758), are dabbling ducks that readily move between water and land, and their behavioral repertoire includes nearly vertical takeoffs in both environments (Raikow, 1973). Consequently, it is likely that mallards also face the challenge of modulating hindlimb movement and muscle function during takeoff depending on the takeoff medium, particularly because the hindlimb contributes to the first part of takeoff when the body is still in contact with the substrate. Previous work on terrestrial takeoff has examined takeoffs from solid surfaces by focusing on distal hindlimb kinematics and substrate reaction forces (Earls, 2000; Tobalske *et al.,* 2004; Berg and Biewener, 2010; Provini *et al*., 2012B; Chin and Lentink, 2017; Crandell *et al.,* 2018) or wing musculature (Williamson *et al.,* 2001). Others have considered behaviors at the water's surface, including paddle-assisted flight (Norberg & Norberg, 1971; Gough *et al.,* 2015), mating displays (Clifton *et al.,* 2015), hydroplaning (Aigeldinger & Fish, 1995), and steaming (Gough *et al.,* 2015). However, no previous studies have examined how vertical takeoff varies between water versus land, and none have reported hindlimb muscle function or the kinematics of proximal joints (hip and knee) during takeoff. Therefore, our goal here is to compare the hindlimb kinematics and *in vivo* function of the lateral gastrocnemius (LG), a major ankle extensor and knee flexor (Biewener and Corning, 2001; Clifton *et al.,* 2018), in response to differences in propulsive requirements for aquatic versus terrestrial takeoffs in mallard ducks.

Similar to other tetrapods that use their hindlimbs for jumping, the hindlimbs play an important role in flight takeoff for many avian species. When taking off from the ground or a perch, birds extend their legs as the wings unfold, with the first downstroke of the wings occurring late in hindlimb extension or after the feet have left the ground or perch (Earls, 2000; Provini *et al.,* 2012B). Depending on the species, the hindlimbs are responsible for 59-100% of the body's velocity at the time of toe-off (Earls, 2000; Tobalske *et al.,* 2004; Berg and Biewener, 2010; Provini *et al*., 2012B; Chin and Lentink, 2017), with the remainder made up by an active upstroke or rotations of the body (Provini *et al*., 2012B).

Because birds take off from a variety of substrates, takeoff performance may be compromised if behaviors are not adjusted to substrate properties (Crandell *et al.,* 2018). Substrate compliance can affect jumping kinematics, with more compliant substrates linked to lower takeoff velocities and larger joint excursions (Giatsis *et al.,* 2004; Astley *et al.,* 2015; Crandell *et al.,* 2018). Waterfowl face perhaps the most disparate tasks of taking off from both terrestrial and aquatic environments. Consequently, adjusting their kinematics to water and land may present challenges for hindlimb muscle tuning.

How locomotor forces are produced necessarily differs between aquatic and terrestrial environments, and these differences can lead to changes in limb kinematics and muscle shortening. On land, an animal's limbs and body are supported and accelerated by ground reaction forces, which are directly proportional to the force produced by skeletal muscles; whereas in water, hydrodynamic forces produced by propulsive appendages (in this case, the duck's feet) accelerate the body and depend on the foot's relative velocity squared (drag force) and on the acceleration of the added mass of fluid displaced by the foot (acceleration reaction force; Daniel, 1984; Biewener and Patek, 2018). Consequently, in order to increase hydrodynamic forces, the duck's feet must be moved faster (H1), requiring greater muscle shortening and contraction velocities (H2). This has particular importance for the function of ankle extensors, such as the LG, which power foot motion. Although active modulation could result in higher hindlimb joint velocities and muscle shortening velocities, the increased compliance of a fluid versus solid substrate can also result in larger limb excursions under a given applied force (Hsieh, 2003; Giatsis *et al.,* 2004), potentially contributing to higher joint excursions and muscle shortening velocities.

How much propulsive force is required differs between terrestrial and aquatic habitats. On land, force must be generated both to support an animal's body weight and to accelerate the body. In contrast, while in water, body weight support is reduced or eliminated due to an animal's buoyancy. However, during aquatic takeoffs, the force required to launch the body is increased by the water's resistance to the bird exiting the water (drag on the body, surface tension) and by water entrained in a bird's plumage, increasing its effective body mass. Nevertheless, we expect that buoyancy will dominate relative to these other forces, resulting in higher forces being required for terrestrial takeoffs (H3). Consistent with this, many animals produce higher forces and increase muscle activation on land compared to in

water (Kamel *et al.,* 1996; Biewener and Gillis, 1999; Gillis & Biewener, 2000; Gillis and Blob, 2001; Foster *et al.,* 2018); although this pattern does not universally hold (Gillis and Blob, 2001). Of most relevance to this study, previous work has shown that the mallard LG produces higher stresses (i.e., force/fiber cross-sectional area) during walking than during surface swimming (Biewener and Corning, 2001).

Thus, we hypothesized that mallard hindlimb kinematics and LG force production would change with takeoff substrate, specifically by producing greater (H1) hindlimb joint extension velocities and (H2) muscle shortening velocities during aquatic takeoffs to generate needed hydrodynamic forces, while producing (H3) greater hindlimb muscle forces during terrestrial takeoffs to accelerate their body and support their weight. Because these differing demands for force versus velocity likely impact hindlimb muscle function, an animal's ability to balance these demands is of particular interest given that skeletal muscles are well known to exhibit a tradeoff between their force and velocity contractile properties (Hill, 1938; McMahon, 1984; Lieber, 1992; Biewener and Patek, 2018). In this study, differences between terrestrial and aquatic takeoffs in mallard ducks were examined by measuring hindlimb kinematics of both proximal and distal joints and *in vivo* function of the LG, a major ankle extensor that generates foot motion during both aquatic and terrestrial locomotion.

Materials & methods

Animals & Training

Wild caught (n=8) and farm-raised (n=4) mallard ducks (Table S1) were fed *ad libitum* and housed in an indoor-outdoor enclosure with both terrestrial and aquatic areas. Experiments were performed during May-November. This period includes a full molt of the primary feathers in late summer that typically renders the ducks flightless for a few weeks. Animals were only studied during times when they had flight ability, either prior to molt or after the feathers had regrown. All animal procedures were approved by Harvard University's Institutional Animal Care and Use Committee under protocol number 20-09. Wild birds were collected under Massachusetts Division of Fisheries & Wildlife Permit 060.15SCB and U.S. Fish & Wildlife Permit MB005348-0.

Birds were trained in the flight arena, a long hall with high ceilings. Training involved first acclimating the birds to two areas: the takeoff area—either a platform (0.6 m x 0.4 m) for terrestrial takeoffs or an acrylic water tank (1m x 1 m x 0.25 m depth) for aquatic takeoff—and the landing area at the other end of the hall. Birds were rewarded with treats (millet) and withdrawal of the researcher when they remained in either location. Researcher approach encouraged the birds to move from the takeoff area to the landing area. A small barrier placed at the front of the platform or tank encouraged vertical takeoffs (Fig. S1A). The barrier height was gradually increased after successful practice trials at previous heights. During all experiments, animals were placed on or guided to the takeoff area. After a period of acclimation (30s-2 min), birds were encouraged to take off by researcher approach, although some birds took off spontaneously. Following takeoff, birds rested in the landing area or were returned to the takeoff area for a rest period of 1-5 minutes.

Animals trained in the flight arena readily translated their training to takeoffs in the X-ray setup, where they took off from the same platform for terrestrial takeoffs as for the light video and from a smaller tank (0.66 m x 0.4 m x 0.3 m depth) for aquatic takeoffs (Fig. S1B). To avoid researcher exposure to the X-ray beam, motion of a glove attached to a long rod was used as a takeoff stimulus.

Kinematics

Timing

We used kinematic parameters to determine when the 'power stroke' of takeoff commenced and ended. All time-varying data, including *in vivo* LG recordings, are plotted relative to the kinematic power stroke, where time=0 is the beginning and time=1 is the end of takeoff power stroke. For terrestrial takeoffs, the first forward and/or upward motion of the body was considered the start of takeoff, with the end of takeoff being when the toe left the ground (i.e., toe-off). For aquatic takeoffs, we considered the first movement of the foot caudally and/or inferiorly as the start of takeoff. During aquatic takeoffs, the webbing of the foot collapses prior to the foot leaving the water, at which point in time the foot likely no longer contributes to powering takeoff as it is drawn forward in the water. We therefore considered collapse of the webbing to be the end of the aquatic takeoff power

stroke. Although normalized time was used to compare relative timing of kinematics and measures of muscle function, real times (s) were used for calculating durations and velocities (joint motion duration, joint angular velocities, muscle shortening velocities, and muscle power).

Ankle & MTP

Takeoffs were elicited in the flight arena, as described above. We used high-speed light video to measure movement of the externally visible portions of the leg (distal tibiotarsus, tarsometatarsus, and foot; Fig. 1A & Movie 1; N=5 individuals, n=15 trials, three trials per individual for each takeoff substrate). Takeoffs were recorded at 250 fps (shutter 1-1.5 ms) using IDT NR5-S1 cameras (Integrated Design Tools, Inc., Pasadena, CA, USA) equipped with Nikon AF Nikkor 24-85 mm zoom lenses (Nikon Inc., Melville, NY, USA). We used a wand of known length to calibrate the 3D space using easyWand5 (Theriault *et al.,* 2014). The tip of the toes, metatarsophalangeal joint (MTP), ankle, and the distal tibiotarsus (Fig. 1A) were marked with white latex and black marker pen, and these points were digitized using DLTdv6 (Hedrick, 2008) to calculate MTP and ankle joint angles. Note that in the example movie (Movie 1), the camera view is oblique rather than perfectly perpendicular since two cameras with a lateral view were used to capture 3D kinematics (Fig. S1A).

Hip & Knee

We used videoradiography to examine the proximal joints for each type of takeoff (N=3 individuals, n=6 trials, two trials per individual for each condition) because these joints are not visible or well-identified using light video. We recorded lateral view X-ray images from a C-arm (Model 9400, OEC-Diasonics Inc.; modified by Radiological Imaging Services) using a high-speed Photron Fastcam 1024 PCI camera (Photron USA, Inc., San Diego, CA, USA, 500 fps, shutter 1 ms). These images were de-distorted using a grid and XMALab (v. 1.4.0; Knörlein *et al.,* 2016).

For terrestrial takeoffs, we performed a 2D analysis using anatomical landmarks to identify the synsacrum, hip, knee, and ankle, so that hip and knee joint angles could be calculated (Fig. 1B). However, the water tank used for aquatic takeoffs was sufficiently

large that the X-ray beam could not penetrate the water, blocking views of the knee and ankle joints. However, the synsacrum and proximal femur were above the water line and thus visible on X-ray video. We combined light video using the IDTs (125 fps) synchronized with the X-ray video to calculate the location and angle of the knee (Fig. 1C). Using a metal calibration object in view of both the light and X-ray videos, the light video of the distal leg was aligned with the X-ray recordings of the proximal leg. 3D coordinates from the light video were then projected onto a plane parallel to the X-ray plane. The X-ray recordings yielded locations for the synsacrum, hip, and the direction of the femur. The light video recordings yielded the location of the ankle and the direction of the tibiotarsus. The locations and angle of the knee were then calculated using these digitized points and measured lengths of the femur and tibiotarsus (Fig. 1C).

Splay Correction for X-ray Analysis

Unlike the 3D analysis used to calculate the ankle and MTP joint angles, the planar X-ray video analysis used to calculate the hip and knee joint angles is susceptible to errors caused by out-of-plane motion (Kambic *et al.,* 2014). Because the mallard femur is splayed relative to the body midline, we measured splay angle (α) for each individual and used it to calculate a duck-specific correction factor. Specifically, we took the x, y coordinates for the synsacrum, hip, knee, and ankle derived from X-ray recordings as described above. We then calculated a z-coordinate (i.e. estimated distance out of plane due to splay) for each point based on splay angle (α) for each individual. The z-coordinate for the synsacrum and hip were set to 0 since they were defined as in-plane. The z-coordinate for the knee was $L_F*\sin(\alpha)$, where L_F is the length of the femur. The z-coordinate for the ankle was represented by z_a. We used the x, y, z coordinates for each point to define the vectors along each bone: synsacrum (S), femur (F), tibiotarsus (T).

$$S = \langle U_S, V_S, W_S \rangle = \langle x_h - x_s, y_h - y_s, 0\text{-}0 \rangle$$

$$F = \langle U_F, V_F, W_F \rangle = \langle x_k - x_h, y_k - y_h, L_F*\sin(\alpha) - 0 \rangle$$

$$T = \langle U_T, V_T, W_T \rangle = \langle x_a - x_k, y_a - y_k, z_a\text{-}L_F*\sin(\alpha) \rangle$$

All of these values could be calculated from known values except for W_T, which was dependent on z_a, which we had not calculated. The magnitude of the T vector is the length of the tibiotarsus (L_T), which we also measured. Thus, we calculated W_T as follows:

$$L_T = \sqrt{(U_T^2 + V_T^2 + W_T^2)}$$

$$W_T = \sqrt{(L_T^2 - U_T^2 - V_T^2)}$$

With all vectors defined, we then calculated the joint angles as the angle between vectors.

$$\Theta_{knee} = 180\text{-}\cos^{-1}[F \bullet T/(L_F * L_T)]$$

$$\Theta_{hip} = \cos^{-1}[S \bullet F/(L_S * L_F)]$$

The splay correction allowed our otherwise 2D analysis to more accurately determine the hip and knee angles. Although unaccounted for out-of-plane motion could produce errors in our measured knee and hip angles, these errors are likely small (i.e., a 10° change in the splay angle would result in < 1° error in the observed angular excursions of the hip and knee joints) and are unlikely to produce changes in kinematic patterns that we observed (see Results).

Filtering

To account for digitizing errors, raw kinematics traces were smoothed in Python (v. 3.7) by applying a 4th order low pass Butterworth filter with a cutoff frequency of 20 Hz for the hip, knee, and ankle joints and 50 Hz for the MTP joint. Kinematics timescales were normalized to the duration of the power stroke, and the data were interpolated in 100 time steps during the power stroke to average across trials and individuals.

In vivo Muscle Measurements:

Surgery

In vivo LG function was measured during aquatic and terrestrial takeoffs in N=10 individuals. We anesthetized (via mask induction) the animals using a 1-2% isoflurane: oxygen gas mixture. Three 2.0 mm sonomicrometry crystals (Sonometrics Corporation, London, Ontario, Canada) were implanted in the LG, one at each end of a mid-belly fascicle and one proximal to, but in-line with, the crystal at the superficial end of the fascicle (Fig. 1). The crystals and lead wires were secured with 5-0 silk suture (Ethicon, Cincinnati, OH, USA). This configuration of crystals allowed us to measure length changes along the fascicle and calculate pennation angle using the law of cosines (Fig. 1D). We also implanted silver fine wire hook electrodes (0.1 mm, with 0.5 mm exposed tips and 2-3 mm spacing, California Fine Wire Company, Grover Beach, CA, USA) to obtain electromyography (EMG)

recordings. An E-shaped tendon buckle was sutured in place on the LG portion of the gastrocnemius tendon, proximal to where the medial gastrocnemius (MG) tendon joins with the LG tendon to form the common tendon (Fig. 1D). The tendon buckle design followed Biewener & Corning (2001) and was built by mounting a strain gauge (Type FLA-1-11, Tokyo Sokki Kenkyujo Co., Ltd., Tokyo, Japan) on the middle arm of an E-shaped piece of 1 mm thick stainless-steel. After soldering 36 gauge lead wires and insulating with oven-cured epoxy (AE-10, Micromeasurements Group, Inc., Raleigh, NC, USA), the transducer was subsequently coated with polyurethane M-coat A (Micromeasurements Group, Inc.) to minimize tissue reaction. All transducer lead wires were passed subcutaneously where they emerged to an external custom-designed 12 pin miniature connector that was secured to the animal's back with 2-0 Vicryl sutures (Ethicon, Cincinnati, OH, USA) between the wings. This connector location allowed us to disconnect the birds from the cables between recording bouts and ensured that the connectors and cables did not inhibit motion of the wings or feet.

Data Collection

Birds were permitted to recover from surgery overnight. Animals were administered flunixin (4 mg kg^{-1}, intramuscularly pectoralis) every 12 hours for the duration of the experiment following surgery (2-3 days). After recovery, we recorded animals performing terrestrial and aquatic takeoffs; takeoffs were elicited as described in the "Animals and Training" section. Signals were transmitted from the animal's back connector via ~8 m shielded multi-lead cable to recording equipment located outside of the flight arena. The sonomicrometry signals were recorded using a Sonometrics Digital Ultrasonic Measurement System (TR-USB Series 8) and sonoLAB data acquisition software (Sonometrics Corporation, London, Ontario, Canada). The tendon buckle signal was passed through a bridge amplifier (Vishay Instruments, Raleigh, NC, USA), and the EMG signals were passed through Grass P-511 Series amplifiers (Grass Instruments, West Warwick, RI, USA) before being recorded at 5000 Hz by a BIOPAC MP150 data acquisition system (BIOPAC Systems, Inc., Goleta, CA, USA) using the accompanying AcqKnowledge software (v. 4.1.1). High-speed light videos of the takeoffs were also recorded as described above. A voltage pulse trigger that illuminated an LED light in the cameras' fields of view was used

to synchronize across software programs and video. This resulted in synchronized kinematics (MTP and ankle joints) and LG force, EMG, fascicle length, and pennation angle. Due to the challenging nature of the experiments, not all data were obtained for all individuals. A list of animals used and the data collected from each is provided in the supplemental information (Table S1).

Following data collection, animals were sacrificed, and the hindlimb was dissected. The tendon force buckle was calibrated by removing the common gastrocnemius tendon from the ankle, distal to the thick fibrocartilage pad. Kevlar thread (DuPont de Nemours, Inc.) was tied proximal to the fibrocartilage pad and attached to a calibrated piezoelectric force transducer (model 9203, Kistler Instrument Corporation, Amherst, NY, USA) or an ergometer lever arm (Aurora Scientific Inc., Aurora, Ontario, Canada). By first freezing the aponeurosis with liquid nitrogen and then pulling on the instrumented tendon or by activating the muscle, we simultaneously recorded the tendon buckle voltage output with the force transducer or lever arm output to obtain dynamic calibrations of tendon force; least-squares linear regression fits had $r^2 > 0.94$ ($p<0.05$). Following calibration, we dissected the hindlimb to confirm the alignment of the sonomicrometry crystals and to measure resting LG fascicle length, resting pennation angle, and muscle mass. The muscle was bisected along the muscle midline, revealing the locations of the implanted sonomicrometry crystals. Length measurements were made with calipers to a precision of 0.1 mm and angles were measured with a swing arm protractor. The distance between the crystals (inter-crystal distance) and the full length of the fascicle in which the crystals were implanted (resting fascicle length) were measured. In order to calculate a mean fascicle length and pennation angle, measurements were taken at 3-6 midline fascicles distributed along the proximo-distal axis of the muscle.

Data Processing

Sonomicrometry crystals were implanted mid-belly to record from as large a portion of the LG muscle's fascicle length as possible (Fig. 1). Measurements of fascicle strain were obtained from the fascicle segment recordings. Resting fascicle length and inter-crystal distance were measured post-mortem, and we multiplied the ratio of these distances (fascicle length/inter-crystal distance) to convert the sonomicrometry output to

fascicle length. Fascicle strain was calculated as (instantaneous length – resting length)/ resting length. Fascicle shortening velocity was calculated from smoothed (4^{th} order low-pass Butterworth filter with 30 Hz cutoff) fascicle length data over the duration of shortening and normalized by resting fascicle length to L s^{-1}.

Muscle-tendon force was filtered using a 4^{th} order low-pass Butterworth filter with a cutoff frequency of 20 Hz. Muscle physiological cross-sectional area (PCSA in cm^2) was calculated as $(\cos(\alpha) * m)/(\rho * l_{fas})$ where α is the pennation angle (Fig. 1), m is muscle mass (kg), ρ is density (assumed to be $1.06 * 10^{-3}$ kg cm^{-3}), and l_{fas} is fascicle length (cm). Muscle stress (kPa) was calculated by dividing force by PCSA. Muscle work (J) was calculated as the area under the force vs. fascicle length curve for the portion of takeoff when both force was being produced and the fascicles were shortening. Work was converted to mass-specific work by dividing by muscle mass. Average mass-specific muscle power was calculated as work / (time * muscle mass).

Statistics

Statistical tests were performed in R (v. 3.6.0). All reported values are mean ± s.e.m., with significance based on $\alpha = 0.05$. We first obtained the average of all measurements for each individual and then plotted and performed statistical tests on the individual averages, which allowed us to account for the different number of trials per individual and/or permitted paired comparisons between aquatic and terrestrial takeoffs. Prior to performing t-tests, normality was verified using a Shapiro-Wilk test. If this assumption was not violated ($p>0.05$), we compared the aquatic and terrestrial takeoffs using one-tailed t-tests. If the normality assumption was violated (Shaprio-Wilk $p<0.05$), we instead used a one-tailed, Wilcoxon nonparametric test. Kinematics were compared using paired tests. LG measurements were compared using unpaired tests. For a subset of animals, we recorded from the LG during both aquatic and terrestrial takeoffs. For some measures with sufficient samples with paired data, we also tested for differences using paired, one-tailed t-tests or Wilcoxon tests, as appropriate, to take into consideration large differences between individuals. All figures display data from all individuals and report paired statistics for kinematics and unpaired statistics for LG measures; any statistics that result from paired tests for LG measures are indicated in the text.

Results

Kinematics during terrestrial versus aquatic takeoffs

The kinematics of aquatic versus terrestrial takeoffs differed substantially (Movie 1). Qualitatively, during terrestrial takeoffs leg extension coincided with wing upstroke and very little overlap with wing downstroke. Many, but not all, terrestrial takeoffs were preceded by a countermovement, where the wings remained folded, legs very flexed, and the head drawn near the body by flexing the neck. The neck began to extend as the wings unfolded and the body angle shifted from horizontal to vertical. Neck extension and shifts in body angle continued throughout the remainder of takeoff. As the legs began to extend, the wings were elevated dorsally and cranially in upstroke. At the point of toe-off, the wings changed direction and were depressed ventrally and slightly caudally for downstroke, the neck was fully extended, and the body angle was nearly vertical. In contrast, during aquatic takeoffs, leg extension coincided with ventral depression of the tail and wing downstroke. Prior to takeoff, the legs were drawn to a very flexed position such that the foot was parallel with and very near to the water's surface. The wings were drawn cranially. The wings were oared through the water with ventral and caudal motion, nearly synchronously with the extension of the leg and ventral depression of the tail. As in terrestrial takeoff, the neck extended and the body angle shifted from horizontal to nearly vertical throughout the takeoff. The wings, tail, and legs reached their final position quickly to propel the bird out of the water; once clear of the water, the wings were elevated dorsally and flapping commenced. The feet also paddled once clear of the water, occasionally striking the water at the surface or, if the water was cleared, cycling mid-air.

Power stroke duration of aquatic takeoffs (0.13 ± 0.018 s) did not differ significantly ($p = 0.087$, Table 1) from terrestrial takeoffs (0.16 ± 0.012 s). Because each limb joint only moves during a portion of the power stroke (Fig. 2), we also compared the duration of motion for each joint, with motion onset based on when joint angular velocity exceeded zero (or fell below zero for the knee during aquatic takeoffs) and motion ending when velocity returned to zero. No significant differences were found for the duration of joint motion between aquatic and terrestrial takeoffs for any of the joints measured ($p > 0.05$, Fig. 3A, Table 1).

Hindlimb kinematics of individual joints differed between terrestrial and aquatic takeoffs. Terrestrial takeoffs involved extension of all hindlimb joints (Fig. 2). In contrast, during aquatic takeoffs hip (Figs 2A & 3B) and MTP (Figs 2D & 3B) joint angles changed very little; angular excursions at these joints were significantly lower than for terrestrial takeoffs (Table 1), resulting in significantly lower angular velocities at these joints during aquatic takeoffs (Fig. 3C, Table 1). The direction of knee motion reversed, with the knee being extended during terrestrial takeoffs but flexed during aquatic takeoffs. This change in direction resulted in significantly different knee angular excursions (Figs 2B & 3B; Table 1) and velocities (Fig. 3C; Table 1), although the magnitudes of the excursion ($p = 0.370$) and velocity ($p = 0.450$) were not different. The ankle underwent a larger angular excursion during aquatic than terrestrial takeoffs (Figs 2C, 3B; Table 1), but no significant difference was observed in ankle extension angular velocity (Fig. 3C; Table 1).

LG function during terrestrial versus aquatic takeoffs

Average time-varying patterns of LG fascicle strain, fascicle shortening velocity, pennation angle, and stress for aquatic and terrestrial takeoff trials are shown in Fig. 4. Representative traces from an individual with nearly complete data sets are shown in Fig. S2, including activation (EMG). A terrestrial trial from a second individual is also displayed, demonstrating the variation in the timing of force production among individuals (Fig. S2). The rapid lengthening of the LG fascicle prior to takeoff (Fig. S2A) corresponds to a countermovement (example in Movie 1). However, because not all animals used a large countermovement, this lengthening pattern is not observed in the LG strain pattern averaged across individuals (Fig. 4A). Similarly, the shortening observed prior to force production for the example terrestrial takeoff (Fig. S2A, black traces) is not observed across all individuals (Figs. 4B, S2A gray traces), and we suspect this shortening results from a shift in body orientation that flexes the knee in preparation for takeoff during this trial. Note that LG fascicles operate at greater strains during aquatic takeoffs due to the extremely flexed position of the ankle joint and, on average, LG stress is higher prior to terrestrial takeoffs due to weight support (Fig. 4). Normalized timing of pennation angle change (terrestrial (T): n=6; aquatic (A): n=5), fascicle shortening (T: n=7; A: n=6), force production (T: n=5; A: n=4), and EMG activity (T: n=6, A: n=2) are shown in Fig. 5A. When

comparing the onset and ending of each of these measures, we found that LG fascicle shortening began later during aquatic takeoffs ($p = 0.022$); whereas, LG force production began earlier ($p = 0.004$) and ended earlier ($p = 0.043$) during terrestrial takeoffs. All other timing parameters, including the onset and ending time of LG pennation angle change and EMG activity, the ending time for fascicle shortening, and the duration of all four measures, did not differ significantly with takeoff medium ($p > 0.05$).

The range of LG fascicle strains used during terrestrial versus aquatic takeoffs are shown in Fig. 5B. When comparing data from all animals (T: n=7; A: n=6), the maximum strains (T: -0.05 ± 0.08; A: 0.15 ± 0.08) and minimum strains (T: -0.27 ± 0.07; A: -0.26 ± 0.06) did not significantly differ between aquatic and terrestrial takeoffs (maximum strain: $p = 0.059$, minimum strain: $p = 0.223$), but both maximum ($p = 0.016$) and minimum fascicle strain ($p = 0.006$) were significantly greater during aquatic takeoffs when based on paired t-tests ($n = 5$). In addition, the magnitude of LG shortening strain was significantly lower ($p = 0.011$) for terrestrial (0.22 ± 0.07) compared with aquatic (0.41 ± 0.06) takeoffs (Fig. 6B). Given the similar shortening durations (Fig. 5A), LG fascicle shortening velocity was also significantly greater ($p = 0.004$) during aquatic (4.12 ± 0.82 L s^{-1}, n=6) versus terrestrial (1.41 ± 0.17 L s^{-1}, n=6) takeoffs (Fig. 6C). Pennation angle change (Fig. 6D) was significantly larger during aquatic takeoffs than terrestrial takeoffs when compared using a paired t-test (difference: 4 ± 1°, $p = 0.018$, n=4), although this difference was not observed when using an unpaired t-test and all animals ($p = 0.127$; T: 10 ± 2°, n=7; A: 15 ± 4°, n=4).

There was not a significant difference in the LG stresses during terrestrial (79 ± 12 kPa) versus aquatic (53 ± 15 kPa) takeoffs ($p = 0.116$; T: n=4, A: n=4; Fig. 6A). LG mass-specific work (T: 8 ± 1 J kg^{-1}; A: 15 ± 5 J kg^{-1}) did not differ significantly between media ($p = 0.1$); however, there was a significant difference ($p = 0.05$) in average muscle power output (T: 43 ± 3 W kg^{-1}; A: 172 ± 72 W kg^{-1}; sample sizes for work and power T: n=3, A: n=3; Fig. 7).

Discussion

Animals that regularly move between aquatic and terrestrial environments must be able to manage the different physical properties of fluids and solids. On land, ground reaction forces are used to support or accelerate an animal's body and are proportional to

443 the forces produced by an animal's muscles. However, in water, propulsive forces are
444 hydrodynamic and depend on the square of the velocity of the body part moving through
445 the water. We, therefore, expected to see differences in both hindlimb kinematics and
446 muscle function of mallards to accommodate differences in environment during takeoff.
447 Specifically, we hypothesized that (H1) hindlimb joints would move at higher angular
448 velocities during aquatic takeoffs than terrestrial takeoffs, that (H2) higher angular
449 velocities at the ankle joint would be powered by higher LG shortening velocities, and that
450 (H3) the LG would produce greater forces during terrestrial than aquatic takeoffs. We did
451 not find support for the hypothesis that mallard hindlimb joints move at higher angular
452 velocities in water (H1, Fig. 3C); however, we did observe substantial differences between
453 the kinematics of aquatic versus terrestrial takeoffs. Of particular interest, the knee
454 reversed its motion from flexion during aquatic takeoffs to extension during terrestrial
455 takeoffs with, unexpectedly, no change in ankle kinematics (Figs. 2 & 3). The change in knee
456 kinematics reflects the underlying difference in LG muscle function, which shortens at
457 higher velocities during aquatic takeoffs than terrestrial takeoffs (H2, Fig. 6C). Finally,
458 although two of the three animals for which we have paired data produced greater muscle
459 stress during terrestrial compared with aquatic takeoffs, overall, the difference in LG
460 muscle stress was not significant (Fig. 6A) and failed to support our hypothesis regarding
461 LG force (H3).
462
463 Takeoff kinematic patterns & implications for muscle length change
464 One way to address the challenge of moving on or through media with differing
465 properties is through different kinematics. Changes in kinematics represent a combination
466 of active control and passive interactions with the environment (Gillis & Biewener, 2000).
467 Our study of takeoff performance, facilitated by X-ray video analysis, confirms
468 changes in mallard hindlimb kinematics, particularly at the knee, between the two media.
469 Knee extension causes cranial motion of the foot while knee flexion and extension at the
470 hip, ankle, and MTP joints cause caudal motion (Fig. 7). The knee joint reverses its direction
471 of rotation, extending during terrestrial takeoffs but flexing during aquatic takeoffs (Figs. 2,
472 3, 7). The overall excursion and angular velocity for each type of takeoff is the same but in
473 opposite directions. Knee flexion during aquatic takeoffs contributes to caudal motion of

474 the foot in the water caused by ankle extension, rather than opposing it (Fig. 7), allowing
475 the knee and ankle joints to work together to enhance foot motion. Similarly, aquatic
476 specialist frog species tend to reduce knee extension during swimming to prevent it from
477 counteracting the propulsive foot motion induced by ankle extension (Richards, 2010). We
478 expect that the change in knee joint rotation was the result of active control, acting to
479 increase foot velocity and hydrodynamic force production. Knee extensors almost certainly
480 contribute to terrestrial takeoff by helping to accelerate the body's center of mass off the
481 ground. Knee flexors (including the LG) likely contribute to knee motion during aquatic
482 takeoff but not terrestrial takeoff. Although the LG is active during both aquatic and
483 terrestrial takeoffs, antagonist activity of knee extensors could prevent the LG from causing
484 knee flexion during terrestrial takeoff.
485 Unexpectedly, the ankle joint exhibited similar kinematics between aquatic and
486 terrestrial takeoffs (Figs. 2 & 3). Although angular excursion of the ankle differed
487 significantly between the two media, the difference was much lower than we observed for
488 the other joints, and ankle angular velocity did not differ significantly. Although this result
489 might suggest that the LG and other muscles driving ankle extension would exhibit similar
490 contractile patterns across both types of takeoff, because the LG crosses both the knee and
491 ankle joints, the reversal in knee motion for aquatic versus terrestrial takeoffs profoundly
492 impacts LG contractile function. During terrestrial takeoffs, the LG shortens to extend the
493 ankle, but this is opposed by knee extension (Fig. 7), resulting in more limited LG
494 shortening and reduced velocity during terrestrial takeoffs (Fig. 6). In contrast, because the
495 knee flexes during aquatic takeoffs, LG shortening is greater and occurs with higher
496 velocities to contribute to knee flexion as well as ankle extension (Fig. 7).
497 Changes in the kinematics of the MTP and hip between terrestrial and aquatic
498 takeoffs likely alter the roles played by the muscles acting at these joints. Both joints
499 undergo large excursions during terrestrial takeoffs but experience almost no angle change
500 during aquatic takeoffs (Figs. 3, 7). The MTP first flexes, as the more proximal joints extend,
501 and then extends rapidly at the end of takeoff from land (Fig. 2). For aquatic takeoffs, MTP
502 motion is negligible, as the joint is held close to 180°, allowing the foot and tarsometatarsus
503 to act as a propulsive paddle. Being held rigid during a power stroke seems to be a
504 characteristic pattern of MTP kinematics for aquatic locomotion, as it is also observed

505 during surface swimming, when flexion of the MTP only occurs during the recovery stroke
506 (Provini *et al.,* 2012A). The hip joint, which exhibits large extensions during terrestrial
507 takeoff, also undergoes little motion during aquatic takeoffs. This pattern is also consistent
508 with other types of avian locomotion, in which the hip undergoes large excursions during
509 walking but is relatively stationary during surface swimming (Carr, 2008; Provini *et al.*,
510 2012A). These hip kinematic patterns are reflected in the length change patterns of hip
511 extensor muscles, which undergo more shortening during walking than during swimming
512 (Carr, 2008). Thus, although we did not measure muscle function at these joints, we would
513 predict that muscles acting at the hip and MTP joints also change roles between aquatic and
514 terrestrial takeoff, with terrestrial takeoffs requiring greater muscle shortening compared
515 with aquatic takeoffs, which would require nearly isometric contractions to stabilize these
516 joints.
517
518 LG stress, work & power
519 Unexpectedly, we observed no significant differences in LG muscle stress or work
520 but did see a significant difference in muscle power output in our *in vivo* recordings across
521 takeoff media (Fig. 6). The small sample size for these variables may have contributed to
522 our inability to distinguish differences that, in fact, exist for muscle stress and work. That
523 muscle work did not differ was perhaps less surprising, given that the increase in muscle
524 shortening during aquatic takeoffs was balanced by a decrease in LG force for two out of
525 the three animals for which paired results were obtained. However, the decrease in LG
526 force observed for most animals was not enough to offset the increase in LG shortening
527 velocity, resulting in significantly higher LG power during aquatic takeoffs.
528 It is interesting to consider how a demanding task like takeoff can be managed by a
529 major leg extensor muscle, such as the LG, which must accommodate differing contractile
530 lengths and velocities depending on the medium in, or on, which the animal moves. Both
531 force-length and force-velocity effects (McMahon, 1984; Lieber, 1992; Biewener & Patek,
532 2018) would decrease the force generating ability of the LG muscle during aquatic takeoffs.
533 Given that LG stress did not decrease significantly, it seems likely that increased neural
534 recruitment compensated for force-length and force-velocity effects. However, our limited

success in obtaining paired EMG recordings of the LG in multiple individuals across both takeoff behaviors (Table S1) prevented us from confirming this.

LG pennation angle changes and muscle gearing

When pennate muscles contract, their fibers can rotate, changing their pennation angle. Fascicle shortening and rotation, therefore, can both contribute to whole muscle shortening (Brainerd and Azizi, 2005; Azizi *et al.,* 2008). The ratio of muscle velocity to fascicle velocity defines a muscle's gear ratio, which has been shown to change in relation to changes in muscle force requirements during shortening contractions (Azizi *et al.,* 2008). Muscle gear ratios are predicted to be higher under low force behaviors, allowing for higher whole muscle shortening velocities, and lower during high force behaviors, keeping the fascicles' force more in line with the line of action of the muscle (Azizi *et al.,* 2008). Consequently, we hypothesized that terrestrial takeoffs would involve lower muscle gear ratios to favor greater force generation, whereas aquatic takeoffs would favor increased gear ratios to enhance whole muscle shortening velocities. Although we did not see a difference in normalized muscle force, or stress, we did observe larger changes in LG pennation angle, consistent with a higher gear ratio, during aquatic takeoffs than terrestrial takeoffs when compared using a paired t-test (Fig. 6).

Implications of moving between water and land

Animals that regularly move between environments face the challenge of using the same propulsive structures and muscles in media having very different physical properties. As made obvious by their webbed feet and waddling gait, many waterfowl, such as mallards, exhibit specializations for swimming that are thought to have compromised their walking ability (Biewener and Corning, 2001; Provini *et al.,* 2012A) and increased the energetic cost of terrestrial locomotion relative to other birds (Pinshow *et al.,* 1977; Griffin and Kram, 2000; Nudds *et al.,* 2010).

As previously discussed, force production varies between environments. On land, animals need to support body weight as well as generate ground reaction forces to accelerate the body. In water, animals produce hydrodynamic forces, which depend on the speed of the propulsive structure (drag) and the acceleration of the added mass of fluid

displaced by the structure (Daniel, 1984). Thus, we predicted that muscle force production would be higher during terrestrial locomotion and joint angular and muscle-shortening velocities would be higher during aquatic locomotion. These hypotheses are consistent with previous comparisons of kinematically similar behaviors where higher muscle EMG activity (Kamel *et al.,* 1996; Biewener and Gillis, 1999; Gillis & Biewener, 2000; Gillis and Blob, 2001; Foster *et al.,* 2018) and higher impulses (Nauwelaerts & Aerts, 2003) are observed during terrestrial locomotion, while faster limb movements are observed during aquatic behaviors (Wilkinson, 2014; Clifton *et al.,* 2015).

That our results don't support these hypotheses is likely a result of their simplicity. For example, we expected the demand for hydrodynamic force would be lower because body weight is supported by buoyancy. However, when moving through water, the ducks also experience other sources of energy loss and demand for force. For example, when taking off from water, the ducks would need to produce force to compensate for drag experienced by the body or accelerating the extra mass of water entrained in the feathers. In addition, as the foot moves faster and hydrodynamic force increases, larger muscle force will be required to balance hydrodynamic force. Thus, velocity and force must simultaneously increase during aquatic locomotion (Richards, 2011), as evidenced by our observation of higher LG power (i.e., force x velocity) during aquatic versus terrestrial takeoffs (Fig. 6).

Another important difference between moving on land versus water is the compliance of water relative to the rigid terrestrial takeoff platform used in our study. Differences in compliance can affect kinematics and performance. For example, takeoff velocity was lower on more compliant substrates for frogs (Astley *et al.,* 2015; Reynaga *et al*., 2019), birds (Crandell *et al.,* 2018), and humans (Giatsis *et al.,* 2004). When jumping from the water column, frogs extended their legs faster than during terrestrial jumps (Wilkinson, 2014) and frogs that reduced slip of their feet during aquatic jumps had higher jump heights (Nauwelaerts *et al.,* 2004). More compliant, dissipative substrates, such as sand, also require more mechanical work and incur a higher energetic cost to walk and run over (Lejeune *et al*., 1998). The higher compliance of a fluid substrate and the resulting 'slip' of the propulsive appendage relative to the fluid also results in a loss of mechanical energy (Hsieh, 2003; Li *et al.,* 2012; Astley *et al.,* 2015; Reynaga *et al.,* 2019), and compromises the

ability of animals to store elastic energy (Li *et al.,* 2012; Reynaga *et al.,* 2019). Because slip (motion of the appendage relative to the fluid) represents energy loss, animals need to produce additional work (Hsieh, 2003; Li *et al.,* 2012) through larger joint excursions or higher forces.

In order to account for differences between environments, ducks are not limited to only changing hindlimb kinematics. Ducks and other waterfowl use their wings and tail to assist foot propulsion during aquatic behaviors, including during vertical takeoffs (Williamson *et al.,* 2001). Although characterizing the contributions of the wings and tail to aquatic takeoff is beyond the scope of the current study, they are clearly key to achieving vertical takeoff in mallards. In fact, the wings and feet working in unison is a common strategy for birds moving at the water's surface and has been described for behaviors like taxiing prior to takeoff or paddle-assisted flight (Norberg & Norberg, 1971; Gough *et al.*, 2015), and hydroplaning and/or steaming (Aigeldinger & Fish, 1995; Gough *et al.,* 2015). An inverse dynamics study pairing ground reaction forces (GRF, measured using a force plate) and fluid dynamic forces (measured using PIV), although challenging to carry out, could elucidate the relative contributions of the hindlimbs, wings, and tail during takeoff. Although not the focus of the current study, preliminary results demonstrated a strong but not significant relationship between GRF and LG stress (r^2=0.88, p=0.06, Fig. S3), suggesting that LG function plays an important role in terrestrial and, we would argue, aquatic takeoffs.

Linked to the kinematic differences they produce, changes in muscle function also facilitate movement in different media. Based on the knee kinematics we observed for aquatic versus terrestrial takeoffs, it is clear that changes in motor coordination patterns must occur, altering the timing of when and which muscles are activated (i.e. knee flexors versus extensors). Differential recruitment of LG synergists could also play a role. Biewener and Corning (2001) observed that the mallard MG contributes equal force compared with the LG during walking but generates much less force during swimming. This suggests that increased MG recruitment may account for the additional force needed to accelerate the body during terrestrial takeoffs, which could explain why we found no significant change in LG stress between terrestrial and aquatic takeoffs.

Because muscle force is maximized over a limited range of length changes and shortening velocities, changes in these parameters could limit force, work, and power production. The LG exhibited higher shortening velocities during aquatic takeoffs than terrestrial takeoffs, which likely compromises its force production for a given amount of muscle recruitment, requiring the recruitment of more fibers and more energy expenditure to produce similar forces. We also observed that the LG operated over longer fascicle lengths and generated force over a broader range of strains during aquatic takeoffs than for terrestrial takeoffs (Fig. 5B), suggesting length-dependent shifts in its force-generating ability. Mapping the LG's *in vivo* muscle use patterns during aquatic and terrestrial takeoff to muscle force-length and force-velocity properties would, therefore, allow us to determine whether these changes in strain and shortening velocity involve a tradeoff in muscle force production.

Conclusions

Locomotion on or through different environments places demands on the mechanisms by which animals generate propulsive forces that require changes in both motor behavior and muscle function. We found that hindlimb kinematics and the function of at least one key propulsive muscle (LG) change between terrestrial and aquatic takeoffs. Because aquatic takeoffs require larger and faster fascicle length changes, LG muscle function is likely altered by changes in neural activation as well as by its intrinsic force-length and force-velocity properties, which may be compensated by differential recruitment of other leg muscles or other parts of the body that assist in propulsion. This study highlights the challenges animals face when moving through or on different media and how muscle function may be tuned across behaviors.

Acknowledgements

We are grateful for the help we received with data collection and analysis, including from Konow Lab at UMass Lowell (especially Dr. Nicolai Konow and Alexandra Collias), Dr. Chris Tijs, Kathryn Gillespie, Kamryn Hoag, Dr. Jennifer Carr, and Jacob Freedman. We appreciate the helpful comments we received from Dr. Tom Roberts on an earlier draft of this manuscript. We are also grateful for the assistance we received from Ken Wilcox and

Pedro Ramirez for help building the experimental setup and providing animal care, respectively, and from the rest of the Concord Field Station community.

Competing Interests

No competing interests declared.

Funding

This work was supported by Harvard University's Department of Organismic & Evolutionary Biology, including through dissertation research funding and the Robert A. Chapman Memorial Scholarship for Vertebrate Locomotion (K.T.-B.).

List of Symbols and Abbreviations

A	Aquatic
EMG	Electromyography
LG	Lateral gastrocnemius
MG	Medial gastrocnemius
MTP	Metatarsophalangeal
PCSA	Physiological cross-sectional area
T	Terrestrial

References

Aigeldinger, T.L. and Fish, F.E. (1995). Hydroplaning by ducklings: overcoming limitations to swimming at the surface. *J. Exp. Biol.* **198:** 1567-1574.

Astley, H.C., Haruta, A. and Roberts, T.J. (2015). Robust jumping performance and elastic energy recovery from compliant perches in tree frogs. *J. Exp. Biol.* **218,** 3360-3363. doi:10.1242/jeb.121715

Azizi, E., Brainerd, E.L. and Roberts, T.J. (2008). Variable gearing in pennate muscles. *Proceedings of the National Academy of Sciences of the United States of America.* **105(5),** 1745-1750.

Berg, A.M. and Biewener, A.A. (2010). Wing and body kinematics of takeoff and landing flight in the pigeon (*Columba livia*). *J. Exp. Biol.* **213,** 1651-1658.

Biewener, A.A. and Corning, W.R. (2001). Dynamics of mallard (*Anas platyrhynchos*) gastrocnemius function during swimming *versus* terrestrial locomotion. *J. Exp. Biol.* **204**, 1745-1756.

Biewener, A.A. and Gillis, G.B. (1999). Dynamics of muscle function during locomotion: accommodating variable conditions. *J. Exp. Biol.* **202,** 3387-3396.

Biewener, A.A. and Patek, S. (2018). *Animal Locomotion, 2nd Ed.* Oxford, UK: Oxford University Press.

Brainerd, E.L. and Azizi, E. (2005). Muscle fiber angle, segment bulging and architectural gear ratio in segmented musculature. *J. Exp. Biol.* **208,** 3249-3261.

Carr, J.A. (2008). Muscle function during swimming and running in aquatic, semi-aquatic, and cursorial birds. *PhD thesis*, Northeastern University, Boston, MA.

Clifton, G.T., Carr, J.A. and Biewener, A.A. (2018). Comparative hindlimb myology of foot-propelled swimming birds. *J. Anat.* **232,** 105-123.

Clifton, G.T., Hedrick, T.L. and Biewener, A.A. (2015). Western and Clark's grebes use novel strategies for running on water. *J. Exp. Biol.* **218,** 1235-1243. doi:10.1242/jeb.118745

Crandell, K.E., Smith, A.F., Crino, O.L. and Tobalske, B.W. (2018). Coping with compliance during take-off and landing in the diamond dove (*Geopelia cuneata*). *PLoS ONE*. **13(7),** e0199662.

Daniel, T. L. (1984). Unsteady aspects of aquatic locomotion. *Am. Zool.* **24,** 121-134.

Earls, K.D. (2000). Kinematics and mechanics of ground take-off in the starling *Sturnis vulgaris* and the quail *Coturnix coturnixi. J. Exp. Biol.* **201,** 725-739.

Foster, K.L., Dhuper, M. and Standen, E.M. (2018). Fin and body neuromuscular coordination changes during walking and swimming in *Polypterus senegalus. J. Exp Biol.* **221,** doi: 10.1242/jeb.168716.

Giatsis, G., Kollias, I., Panoutsakopoulos, V. and Papaiakovou, G. (2004). Volleyball: Biomechanical differences in elite beach-volleyball players in vertical squat jump on rigid and sand surface. *J. Sports Biomechanics.* **3,** 145-158. DOI: 10.1080/14763140408522835

Gillis, G.B. and Biewner, A.A. (2000). Hindlimb extensor muscle function during jumping and swimming in the toad (*Bufo marinus*). *J. Exp. Biol.* **203,** 3547-3563.

Gillis, G.B. and Blob, R.W. (2001). How muscles accommodate movement in different physical environments: aquatic vs. terrestrial locomotion in vertebrates. *Comparative Biochemistry and Physiology Part A.* **131,** 61-75.

Gough, W.T., Farina, S.C., and Fish, F.E. (2015). Aquatic burst locomotion by hydroplaning and paddling in common eiders (*Somateria mollissima*). *J. Exp. Biol.* **218:** 1632-1638.

Griffin, T.M. and Kram, R. (2000). Penguin waddling is not wasteful. *Nature.* **408,** 929.

Hedrick, T.L. (2008). Software techniques for two- and three-dimensional kinematic measurements of biological and biomimetic systems. *Bioinspri. Biomim.* **3(3)**, 034001.

Hill, A. V. (1938). The heat of shortening and the dynamic constants of muscle. *Proc. Roy. Soc. Lond. B,* **126**, 136-195.

Hsieh, S.T. (2003). Three-dimensional hindlimb kinematics of water running in the plumed basilisk lizard (*Basiliscus plumifrons*). *J. Exp. Biol.* **206,** 4363,4377.

Kambic, R.E., Roberts, T.J. and Gatesy, S.M. (2014). Long-axis rotation: a missing degree of freedom in avian bipedal locomotion. *J. Exp. Biol.* **217,** 2770-2782 doi:10.1242/jeb.101428

Kamel, L.T., Peters, S.E. and Bashor, D.P. (1996). Hopping and swimming in the leopard frog, *Rana pipiens*: II. A comparison of muscle activities. *J. Morphol.* **230,** 17-31.

Knörlein, B.J., Baier, D.B., Gatesy, S.M., Laurence-Chasen, J.D. and Brainerd, E.L. (2016). Validation of XMALab software for marker-based XROMM. *J. Exp. Biol.* **219**, 3701-3711.

Lejeune, T. M., Willems, P. A., and Heglund, N. C. (1998). Mechanics and energetics of human locomotion on sand. *J. Exp. Biol.* **201,** 2071-2080.

Li, C., Hsieh, S.T. and Goldman, D.I. (2012). Multi-functional foot use during running in the zebra-tailed lizard (*Callisaurus draconoides*). *J. Exp. Biol.* **215,** 3293-3308.

Lieber, R. L. (1992). *Skeletal Muscle Structure and Function.* Baltimore, MD: Williams and Wilkins.

Maladen, R.D., Ding, Y., Li, C. and Goldman, D.I. (2009). Undulatory swimming in sand: subsuraface locomotion of the sandfish lizard. *Science.* **325,** 314-318. (DOI: 10.1126/science.1172490)

McMahon, T. A. (1984). *Muscles, Reflexes, and Locomotion.* Princeton, N.J.: Princeton Univ. Press.

Nauwelaerts, S. and Aerts, P. (2003). Propulsive impulse as a covarying performance measure in the comparison of the kinematics of swimming and jumping in frogs. *J. Exp. Biol.* **206,** 4341-4351.

Nauwelaerts, S., Scholliers, J. and Aerts, P. (2004). A functional analysis of how frogs jump out of water. *Biological Journal of the Linnean Society.* **83,** 413-420.

Norberg, R.A. and Norberg, U.M. (1971). Take-off, landing, and flight speed during fishing flights of *Gavia stellate* (Pont.). *Ornis Scan.* **2,** 55-67.

Nudds, R.L., Gardiner, J.D., Tickle, P.G. and Codd, J.R. (2010). Energetics and kinematics of walking in the barnacle goose (*Branta leucopsis*). *Comparative Biochemistry & Physiology, Part A.* **156**, 318-324.

Peters, S.E., Kamel, L.T. and Bashor, D.P. (1996). Hopping and swimming in the leopard frog, *Rana pipiens*: I. Step cycles and kinematics. *J. Mophol.* **230,** 1-16.

Pinshow, B., Fedak, M.A. and Schmidt-Nielsen, K. (1977). Terrestrial locomotion in penguins: it costs more to waddle. *Science*. **195,** 592-594.

Provini, P., Goupil, P., Hugel, V. and Abourachid, A. (2012A). Walking, paddling, waddling: 3d kinematics Anatidae locomotion (*Callonetta leucophrys*). *J. Exp. Zool.* **317,** 275-282.

Provini, P., Tobalske, B.W., Crandell, K.E. and Abourachid, A. (2012B). Transition from leg to wing forces during take-off in birds. *J. Exp. Biol.* **215,** 4115-4124.

Raikow, R.J. (1973). Locomotor mechanisms in North American ducks. *The Wilson Bulletin*. **85(3)**, 295-307.

Reynaga, C.M., Eaton, C.E., Strong, G.A. and Azizi, E. (2019). Compliant substrates disrupt elastic energy storage in jumping tree frogs. *Int. Comp. Bio.* **59,** 1535-1545.

Richards, C.T. (2010). Kinematics and hydrodynamics analysis of swimming anurans reveals striking inter-specific differences in the mechanisms for producing thrust. *J. Exp. Biol.* **213,** 621-634.

Richards, C.T. (2011). Building a robotic link between muscle dynamics and hydrodynamics. *J. Exp. Biol.* **214,** 2381-2389. doi:10.1242/jeb.056671

Sharpe, S.S., Ding, Y. and Goldman, D.I. (2013). Environmental interaction influences muscle activation strategy during sand-swimming in the sandfish lizard *Scincus scincus*. *J. Exp. Biol.* **216,** 260-274.

Theriault, D.H., Fuller, N.W., Jackson, B.E., Bluhm, E., Evangelista, D., Wu, Z., Betke, M. and Hedrick, T.L. (2014) A protocol and calibration method for accurate multi-camera field videography. *J. Exp. Biol.* **217**, 1843-1848; doi: 10.1242/jeb.100529

Wilkinson, K.C. (2014). A kinematic and kinetic analysis of a frog launching from water using digital particle image velocimetry. *MS thesis*, Northern Arizona University, Flagstaff, AZ.

Williamson, M.R., Dial, K.P. and Biewener, A.A. (2001). Pectoralis muscle performance during ascending and slow level flight in mallards (*Anas platyrhynchos*). *J. Exp. Biol.* **204,** 495-507.

Winter, D.A. (1990). *Biomechanics and Motor Control of Human Movement, 2nd Ed.* New York, USA: John Wiley & Sons, Inc.

Tables

Table 1. Comparisons of total power stroke duration and hindlimb joint motion duration, angular excursion, and velocity by joint during terrestrial and aquatic takeoffs.

	Duration (s)	Angular Excursion (°)	Angular Velocity (° s^{-1})
Total Power Stroke			
Terrestrial	0.16 ± 0.012		
Aquatic	0.13 ± 0.018		
p-value	0.087		
Hip			
Terrestrial	0.170 ± 0.024	54.8 ± 9.3	375 ± 26
Aquatic	0.109 ± 0.069	20.6 ± 3.7	257 ± 53
p-value	0.234	**0.016**	**0.038**
Knee			
Terrestrial	0.091 ± 0.035	36.4 ± 4.7	421 ± 48
Aquatic	0.116 ± 0.036	-38.5 ± 11.5	-406 ± 143
p-value	0.462	**0.022**	**0.024**
Ankle			
Terrestrial	0.102 ± 0.021	72.6 ± 18.3	840 ± 414
Aquatic	0.105 ± 0.027	92.8 ± 10.7	979 ± 316
p-value	0.853	**0.031**	0.238
MTP			
Terrestrial	0.028 ± 0.003	56.2 ± 5.0	2120 ± 340
Aquatic	0.021 ± 0.008	13.8 ± 23.6	870 ± 851
p-value	0.149	**0.011**	**0.022**

Bolded p-values indicate that the paired, one-way t-test showed a significant difference between aquatic and terrestrial takeoffs.

Figure Captions

Figure 1. Methods for measuring joint angle changes (A-C) and LG function (D). (A-C) The key applies to panels A-C. The digitized points (indicated) were used to calculate joint angle change. (A) Markers on the tibiotarsus, ankle, MTP, and toe were visible in light video and were used to calculate ankle and MTP joint angles. (B) During terrestrial takeoff, anatomical landmarks on synsacrum, hip, femur, knee, and ankle were visible in X-ray video. These points were used to calculate knee and hip angles. (C) During aquatic takeoffs, the hip joint angle was calculated as in (B), but the water blocked the X-ray visualization of distal points. Instead, we combined light visualization of the ankle and tibiotarsus and X-

848 ray visualization of the hip and femur. The projected directions of the tibiotarsus and femur
849 were used to find the intersection of these bones (i.e., the knee) based on their measured
850 lengths. Knee angle was calculated using the calculated knee position. (D) Schematic of a
851 lateral view of the left hind leg with electrodes implanted to measure *in vivo* LG function.
852 An outline of the hind leg is shown in light gray and the bones are shown in dark gray. The
853 LG (pink) is a longitudinal cross-section, showing the placement of the sonomicrometry
854 crystals (white circles) used to measure length of a fascicle segment ($L_{fas,\,seg}$) and pennation
855 angle. The location of the EMG electrodes is shown (x) but electrodes were placed medially
856 or laterally to the sonomicrometry plane, not in the same plane. Placement of the tendon
857 buckle (black E shape) on the LG tendon to measure LG forces is also shown.
858
859 Figure 2. Hindlimb joint kinematics differ for aquatic versus terrestrial takeoffs. (A) Hip,
860 (B) knee, (C) ankle, and (D) MTP joint angles (mean (solid line) $\pm$ s.e.m. (shading)) during
861 aquatic (blue) and terrestrial (black) takeoff plotted against the proportion of the takeoff
862 power stroke, as determined by kinematic analysis (see methods for more detail). Hip and
863 knee angles were calculated from two trials each for three individuals (n=6 trials) for
864 aquatic and terrestrial takeoffs. Ankle and MTP averages were calculated for three trials for
865 each condition from five individuals (n=15 trials).
866
867 Figure 3. Kinematic parameters varied between aquatic and terrestrial takeoffs for some
868 joints but not others. Comparisons by joint of (A) duration of movement, (B) angle changes,
869 and (C) angular velocity during aquatic (blue) and terrestrial (white) takeoffs. Boxplots
870 show the median (thick line), upper and lower quartiles, and highest and lowest values
871 (vertical lines), excluding outliers. Hip and knee angles were calculated from two trials
872 each for three individuals (n=6 trials) for aquatic and terrestrial takeoffs. Ankle and MTP
873 averages were calculated for three trials for each condition from five individuals (n=15
874 trials). Significant differences found using one-tailed t-tests or Wilcoxon tests are denoted
875 (*, $p < 0.05$; see Table 1).
876
877 Figure 4. LG muscle function differs between aquatic and terrestrial takeoffs. Mean (solid
878 lines) ± s.e.m. (shaded regions) time varying patterns of LG (i) fascicle strain (T: n=6, A:

879 n=6), (ii) fascicle velocity (T: n=6, A: n=5), (iii) pennation angle (T: n=6, A: n=5), and (iv)
880 stress during (T: n=4, A: n=4) (A) terrestrial and (B) aquatic takeoffs. Data are plotted
881 against the proportion of takeoff, with the start and stop times of takeoff determined from
882 kinematics (see methods for more detail). The gray box indicates the power stroke of
883 takeoff. Negative velocities indicate fascicle lengthening while positive velocities indicate
884 fascicle shortening.
885
886 Figure 5. LG timing parameters and length changes vary between takeoff media. (A)
887 Relative timing of changes in pennation angle (terrestrial (T): n=6, aquatic (A): n=5),
888 fascicle shortening (T: n=7; A: n=6), force production (T: n=5; A: n=4), and EMG activity T:
889 n=6, A: n=2). Times are compared using unpaired one-tailed t-tests or Wilcoxon tests.
890 Force production began ($p=0.004$) and ended ($p=0.043$) significantly earlier during
891 terrestrial takeoffs. Shortening also began earlier during terrestrial takeoffs ($p=0.022$). All
892 other start and end times and durations were not significantly different ($p>0.05$). (B) LG
893 fascicle strains (i.e., normalized lengths) observed during aquatic versus terrestrial takeoffs.
894 Maximum strain ($p=0.059$) and minimum strain ($p=0.223$) were not significantly different
895 when considering all animals (T: n=7; A: n=6, data shown), but both the maximum strain
896 ($p=0.016$) and minimum strain ($p=0.006$) were larger for aquatic takeoffs versus terrestrial
897 takeoffs in animals for which we have paired data (n=5), using a paired t-test. Values are
898 mean ± s.e.m.
899
900 Figure 6. *In vivo* LG function differs for some key contractile parameters between aquatic
901 and terrestrial takeoffs. Boxplots showing LG (A) stress (T: n=4 individuals; A: n=4), (B)
902 shortening strain (T: n=7, A: n=6), (C) shortening velocity (T: n=6; A: n=6), (D) pennation
903 angle change (T: n=7; A: n=4), and mass-specific (E) work and (F) power (T: n=3; A: n=3)
904 for aquatic (blue) and terrestrial (black) takeoffs. Whereas muscle stress did not differ
905 significantly ($p=0.116$), fascicle shortening strain ($p=0.011$) and velocity ($p=0.004$) were
906 significantly larger for aquatic versus terrestrial takeoffs. Pennation angle change was not
907 significantly different when compared using an unpaired t-test ($p=0.127$, plotted above)
908 but pennation angle change was significantly larger during aquatic takeoffs than terrestrial
909 takeoffs when compared using a paired t-test ($p=0.018$, n=4). Work was not significantly

910 different between takeoff media (p=0.2), but power was significantly higher during aquatic
911 takeoffs (p=0.05). Boxplots show the median (thick line), upper and lower quartiles, and
912 highest and lowest values (vertical lines), excluding outliers. Averages for individual ducks
913 are shown as open circles. Significant differences between aquatic (blue) versus terrestrial
914 (black) takeoffs found using 1-tailed t-tests or Wilcoxon tests are denoted (*, $p < 0.05$; see
915 Table 1).
916
917 Figure 7. Knee and ankle kinematics have implications for LG function. (A) For clarity,
918 whole-hindlimb takeoff kinematics are plotted holding the toe (terrestrial, Ai) or hip
919 (aquatic, Aii) stationary. The joint angle at the beginning of takeoff are shown in light
920 gray/blue for the beginning of takeoff and dark gray/black for the end of takeoff. During
921 terrestrial takeoffs, the knee and ankle extend, helping to accelerate the body. During
922 aquatic takeoff, knee flexion and ankle extension both contribute to backward motion of
923 the foot. (B) A simplified model of the femur, tibiotarsus, and tarsometatarsus are shown,
924 The LG is represented by the red/pink bands, with the origin and insertion (circles)
925 locations exaggerated for clarity. For ease of comparison, the tibiotarsus is held stationary.
926 The segment/muscle positions are light gray/pink for the beginning of takeoff and
927 black/red for the end of takeoff. During terrestrial takeoff, ankle extension is caused by LG
928 shortening, but knee extension tends to counteract this motion, decreasing LG strain and
929 shortening velocity. During aquatic takeoff, knee flexion and ankle extension are both
930 linked to LG shortening, resulting in higher strains and shortening velocities in the LG.

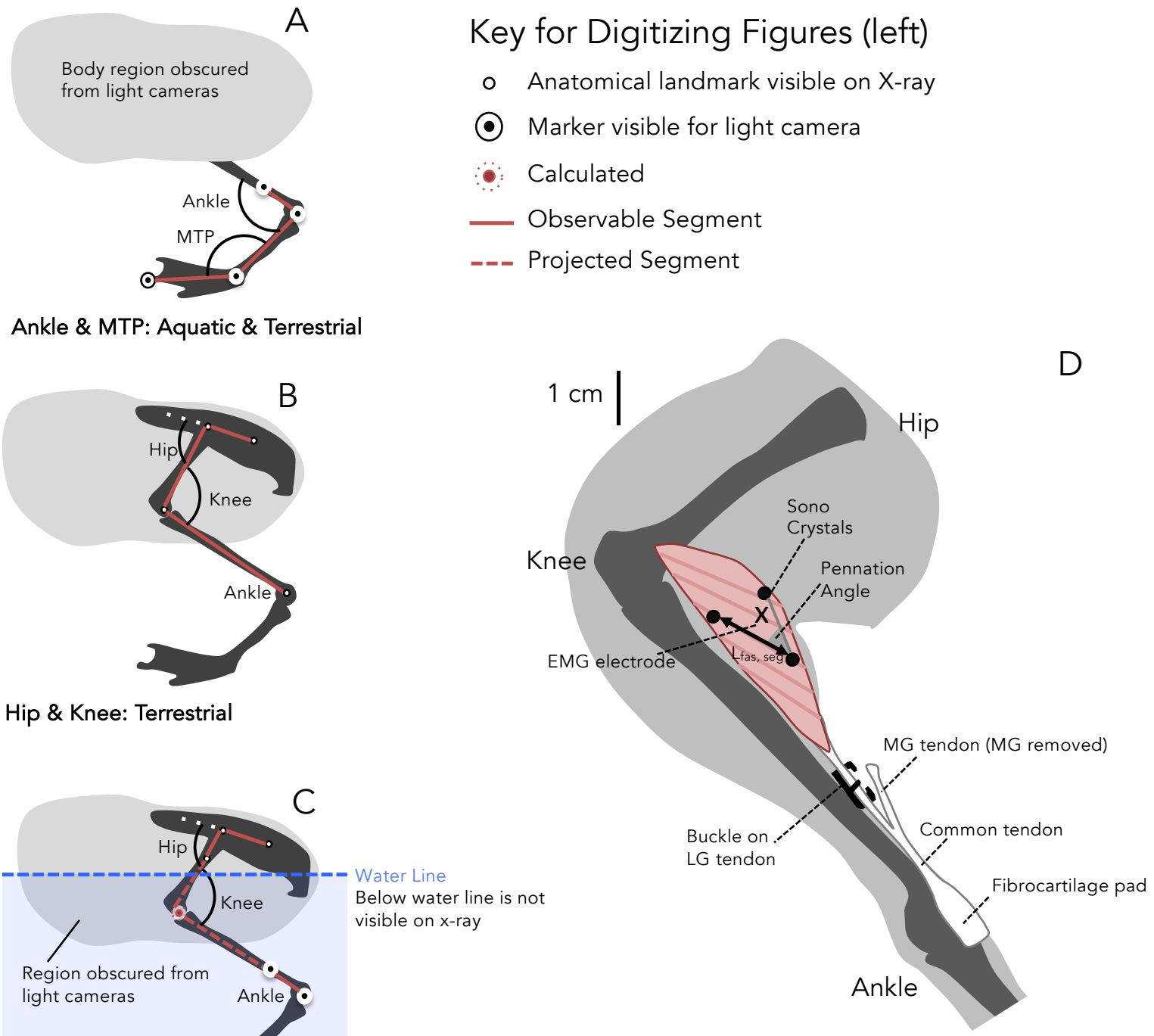
A
Body region obscured from light cameras
Ankle
MTP
Ankle & MTP: Aquatic & Terrestrial
Key for Digitizing Figures (left)
Anatomical landmark visible on X-ray
Marker visible for light camera
Calculated
Observable Segment
Projected Segment
B
Hip
Knee
Ankle
Hip & Knee: Terrestrial
C
Hip
Knee
Water Line
Below water line is not visible on x-ray
Region obscured from light cameras
Ankle
Hip & Knee: Aquatic
D
1 cm
Hip
Knee
Sono Crystals
Pennation Angle
X
EMG electrode
L fas, seg
MG tendon (MG removed)
Common tendon
Buckle on LG tendon
Fibrocartilage pad
Ankle

Figure 1

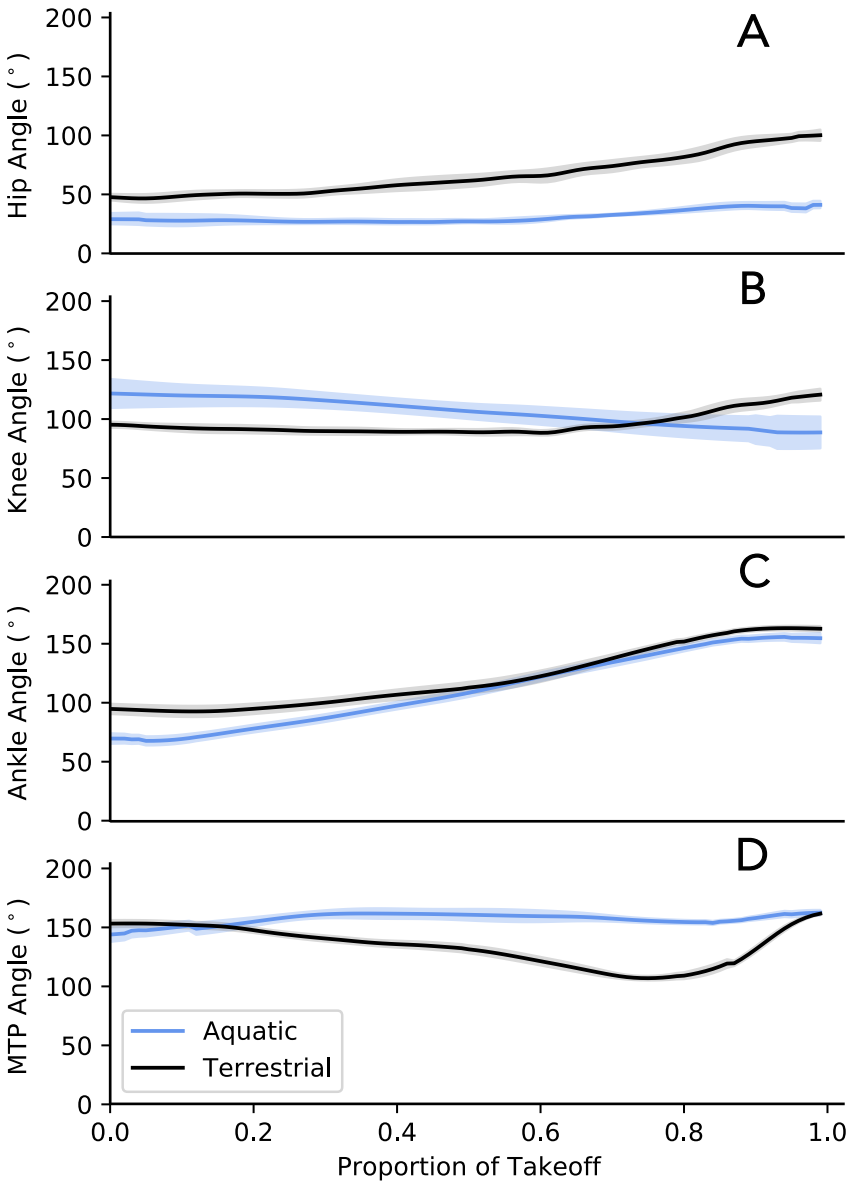
A
B
C
D
Hip Angle (°)
Knee Angle (°)
Ankle Angle (°)
MTP Angle (°)
200
150
100
50
0
Aquatic
Terrestrial
0.0
0.2
0.4
0.6
0.8
1.0
Proportion of Takeoff

Figure 2

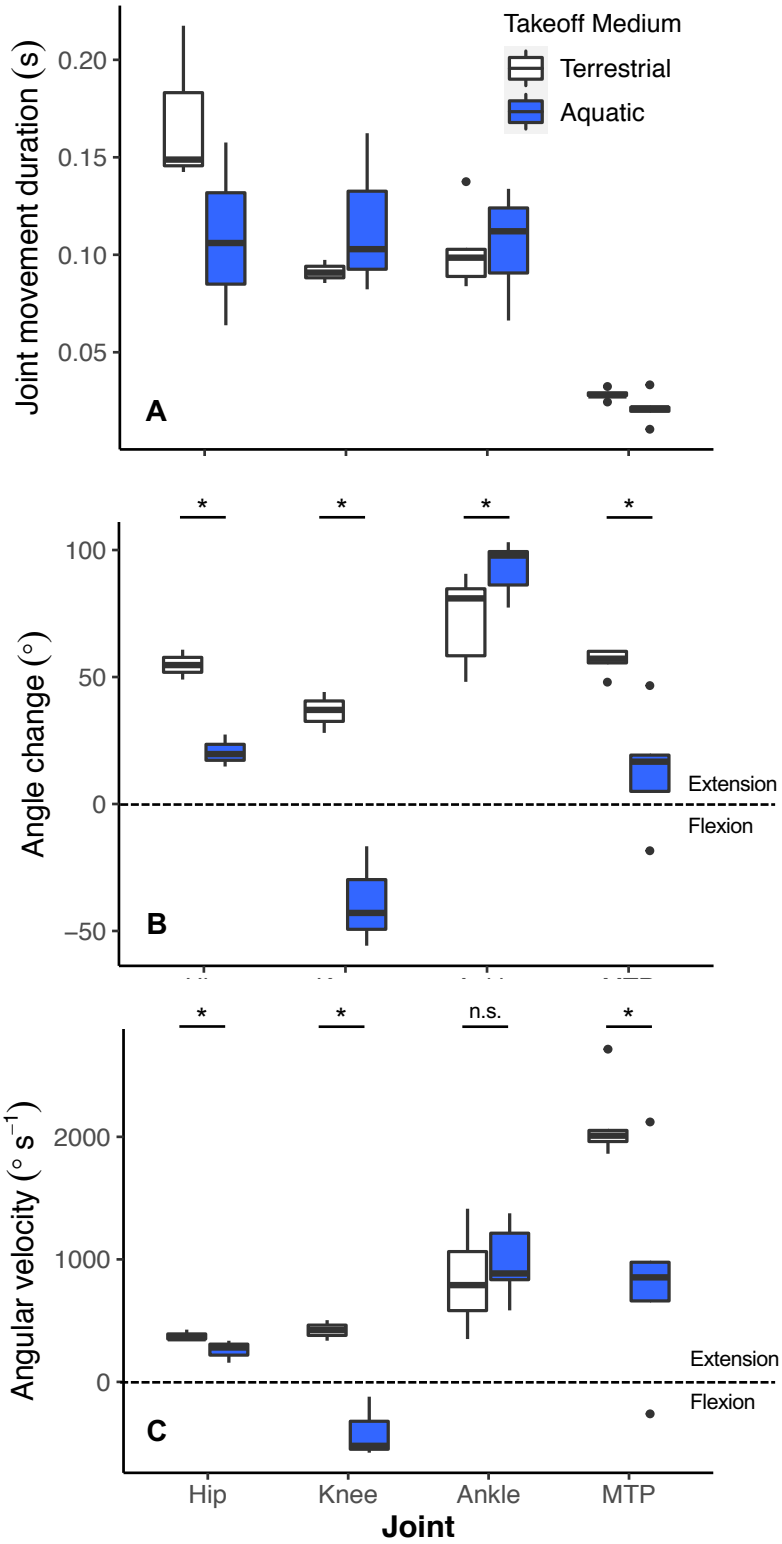
Takeoff Medium
Terrestrial
Aquatic
Joint movement duration (s)
0.20
0.15
0.10
0.05
A
*
*
*
*
Angle change (°)
100
50
0
−50
Extension
Flexion
B
*
*
n.s.
*
Angular velocity (° s^{-1})
2000
1000
0
Extension
Flexion
C
Hip
Knee
Ankle
MTP
Joint

Figure 3

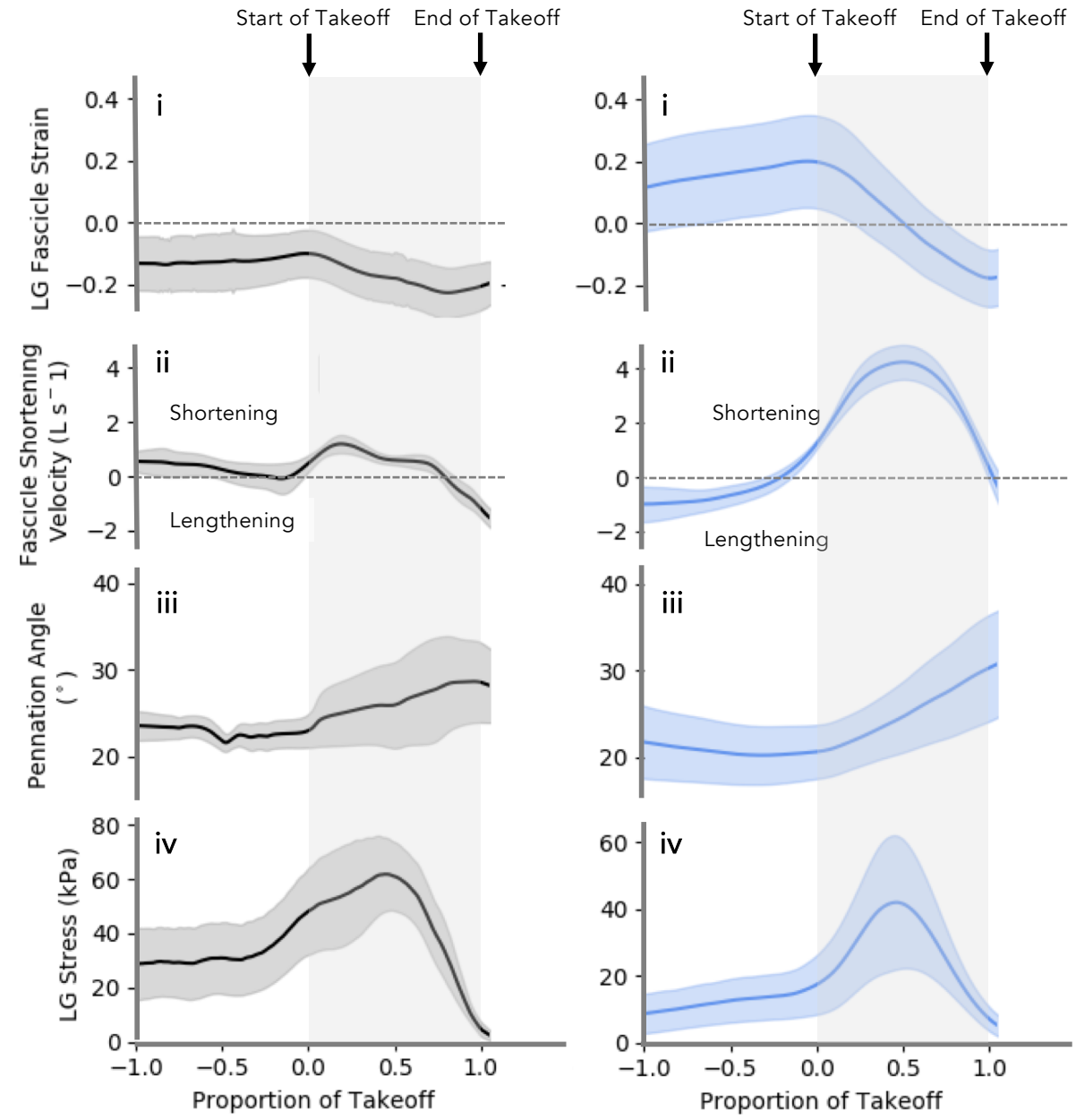
A. Terrestrial
B. Aquatic
Start of Takeoff
End of Takeoff
LG Fascicle Strain
Fascicle Shortening Velocity (L s⁻¹)
Pennation Angle (°)
LG Stress (kPa)
i
ii
iii
iv
Shortening
Lengthening
Proportion of Takeoff

Figure 4

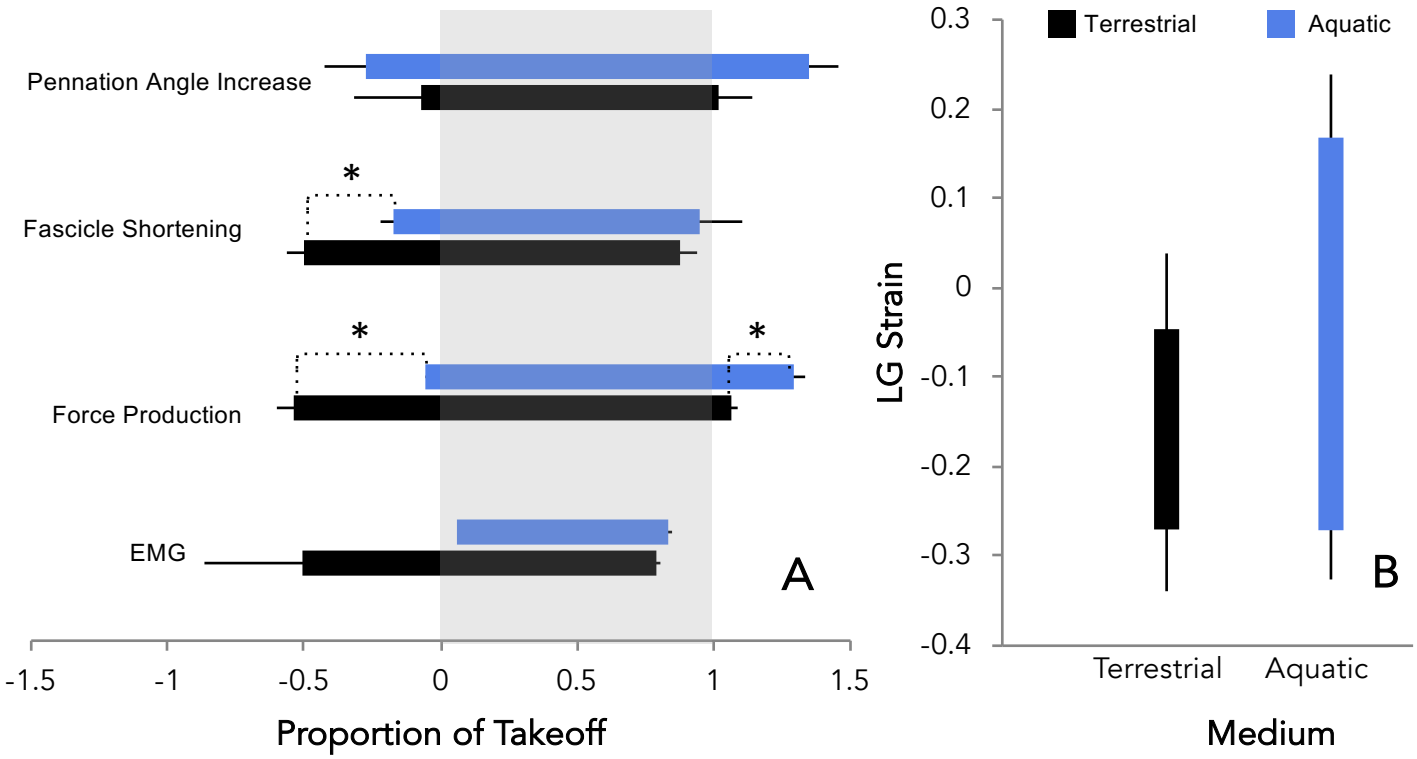
Pennation Angle Increase
Fascicle Shortening
Force Production
EMG
*
*
*
A
-1.5
-1
-0.5
0
0.5
1
1.5
Proportion of Takeoff
0.3
0.2
0.1
0
-0.1
-0.2
-0.3
-0.4
LG Strain
Terrestrial
Aquatic
B
Terrestrial
Aquatic
Medium

Figure 5

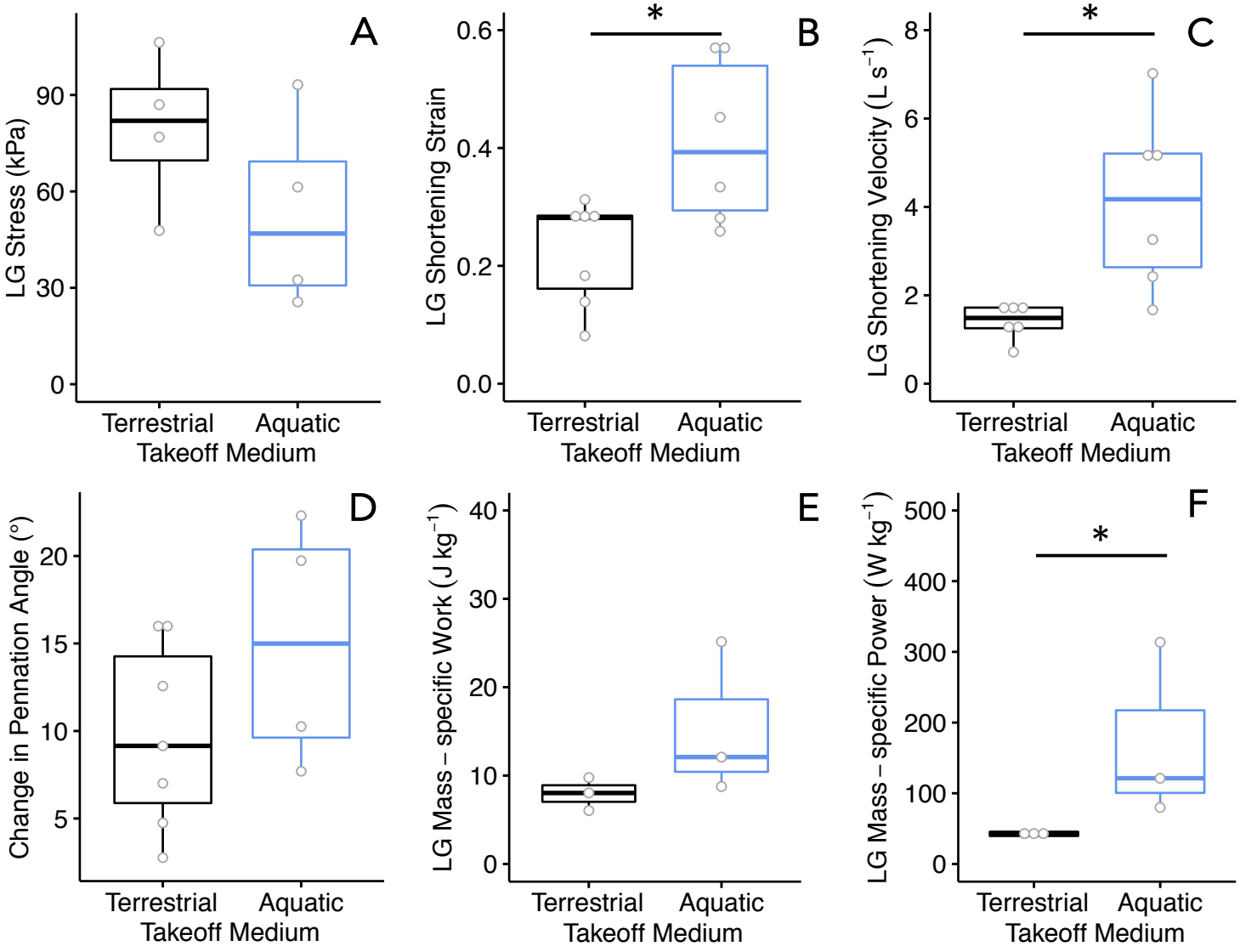
A
LG Stress (kPa)
0
30
60
90
Terrestrial
Aquatic
Takeoff Medium
B
*
LG Shortening Strain
0.0
0.2
0.4
0.6
Terrestrial
Aquatic
Takeoff Medium
C
*
LG Shortening Velocity (L s^{-1})
0
2
4
6
8
Terrestrial
Aquatic
Takeoff Medium
D
Change in Pennation Angle (°)
5
10
15
20
Terrestrial
Aquatic
Takeoff Medium
E
LG Mass – specific Work (J kg^{-1})
0
10
20
30
40
Terrestrial
Aquatic
Takeoff Medium
F
*
LG Mass – specific Power (W kg^{-1})
0
100
200
300
400
500
Terrestrial
Aquatic
Takeoff Medium

Figure 6

A. Kinematics

B. LG Function

i. Terrestrial

Knee extension and ankle extension both help to launch the body. However, these joint actions oppose each other, resulting in lower LG shortening strains as the LG shortens to extend the ankle but lengthens as the knee extends.

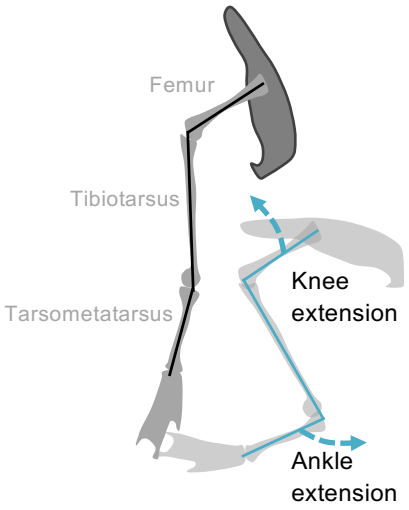

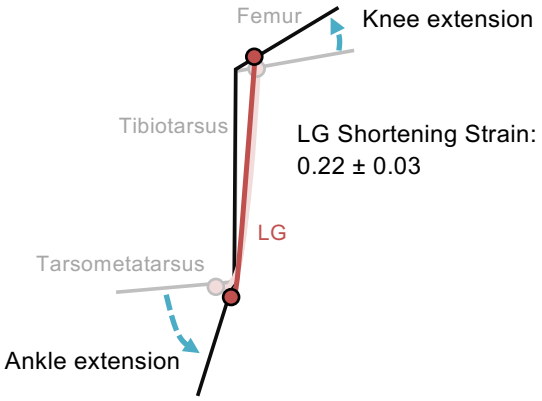

ii. Aquatic

Knee flexion and ankle extension both contribute to backward motion of the foot.

Both motions are powered by large shortening strains and high shortening velocity by the LG.

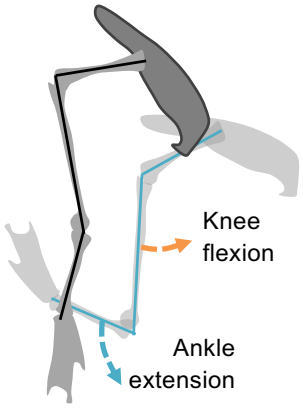

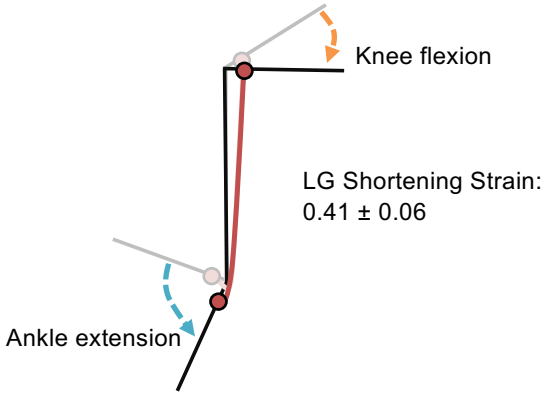

Figure 7

Supplemental Information: Aquatic and terrestrial takeoffs require different hindlimb kinematics and muscle function in mallard ducks
K.R. Taylor-Burt & A.A. Biewener

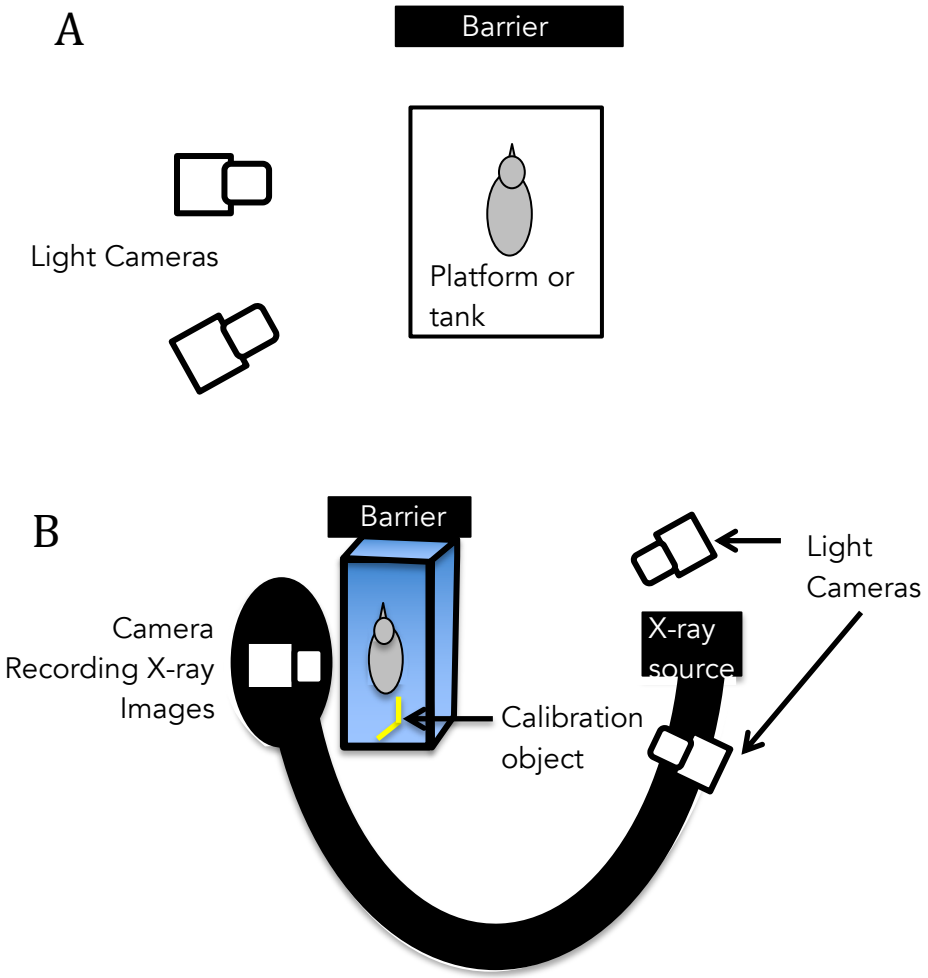

Figure S1. Methods for recording joint angle changes during aquatic and terrestrial takeoffs. (A) Light video camera only setup. This setup was used to measure ankle and MTP joint movement. Ducks were recorded at 250 fps as they took off from platform or tank over a barrier. (B) X-ray video setup used to measure hip and knee joints. For terrestrial takeoffs, ducks took off from a platform and hip and knee were measured from X-ray video. For aquatic takeoff, ducks took off from a tank. Hip angles were measured from the X-ray video. Knee angles were calculated using a 2D light and X-ray setup.

Supplemental Information: Aquatic and terrestrial takeoffs require different hindlimb kinematics and muscle function in mallard ducks
K.R. Taylor-Burt & A.A. Biewener

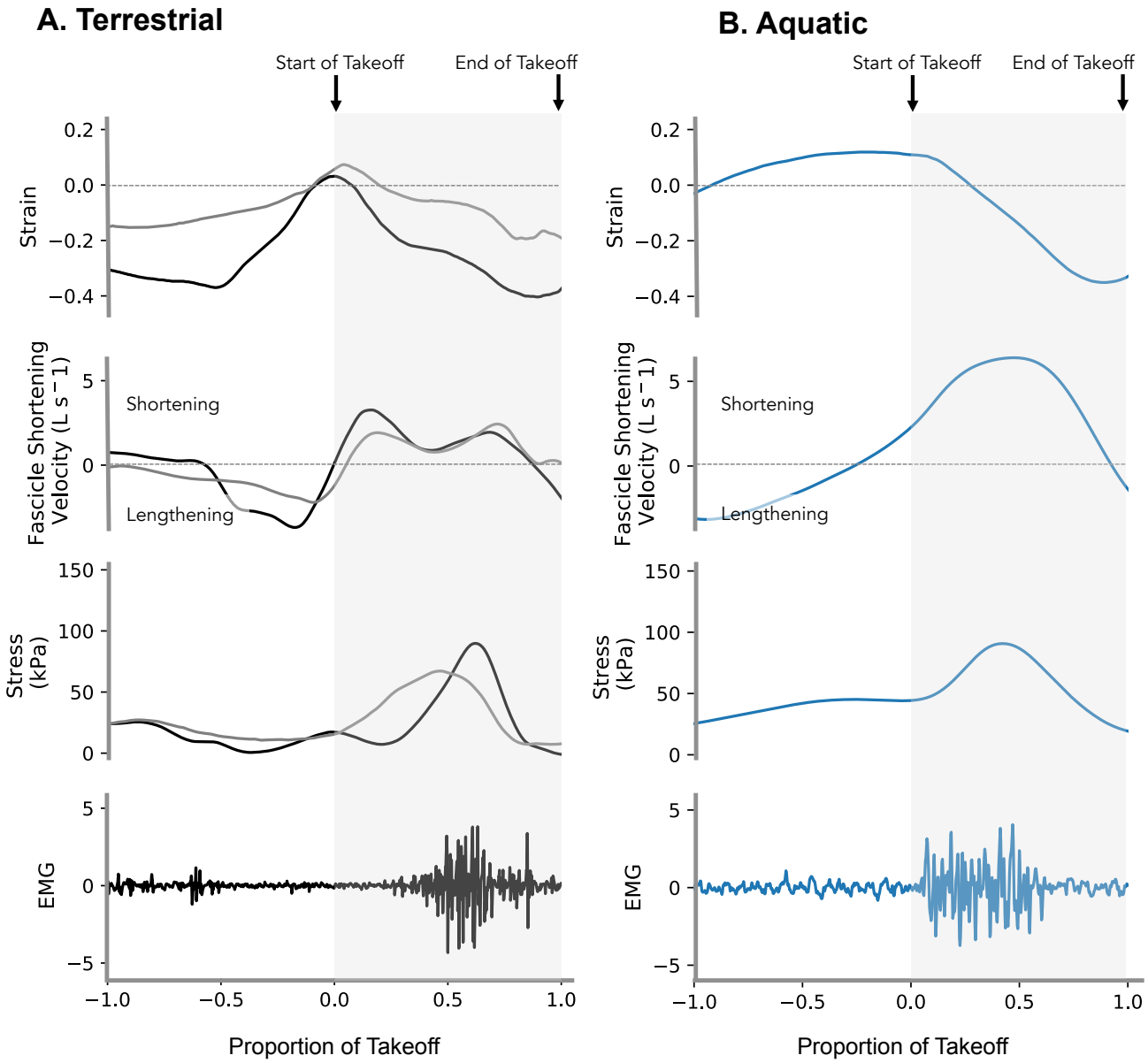

Figure S2. Example fascicle strain, shortening velocity, muscle stress, and EMG recorded from the LG of one duck during an (A) terrestrial (black) and (B) aquatic (blue) takeoff. Example fascicle length, fascicle velocity, and stress during terrestrial takeoff are shown for a second individual (gray) to illustrate the variation in timing of force production. Data are plotted against the proportion of takeoff, with the start and stop times of takeoff determined from kinematics (see methods for more detail). The gray box indicates the takeoff power stroke. Negative velocity indicates muscle lengthening and positive velocity indicates muscle shortening. Pennation angle

data were not available for these animals; however, average patterns across ducks, including for pennation angle, are shown in Fig. 4.

Movie 1. Example terrestrial and aquatic takeoff in light video setup (Fig. S1). Note: two cameras were used at oblique angles to provide 3D kinematics and so may not be perfectly perpendicular to the animal's motion.

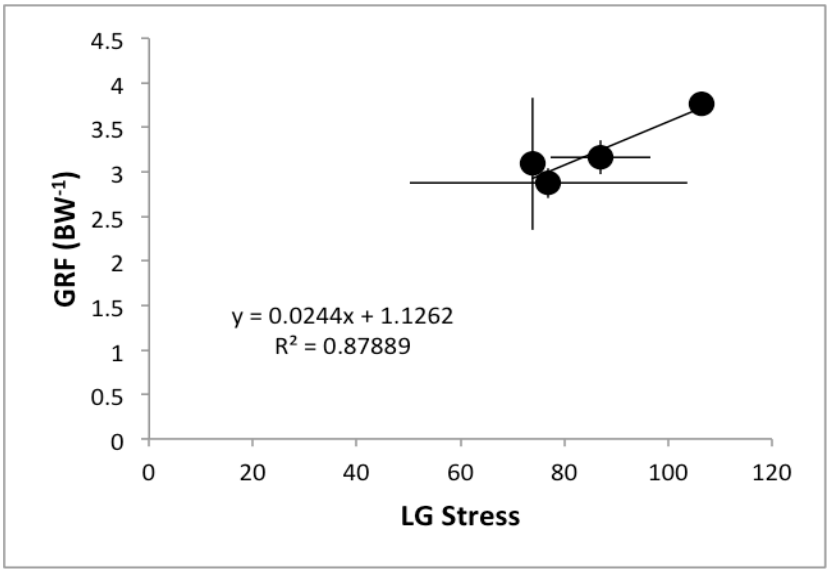

Figure S3. Preliminary force plate analysis results. Ground reaction force (GRF) vs. LG stress measured during terrestrial takeoffs (N=4 animals, n=10 trials). Points are individual averages. GRF was measured as the vector sum of vertical and fore-aft forces (mediolateral forces were assumed to be negligible). Stress was calculated as described in the Methods section. The magnitude of GRF was normalized by body weight (BW). The mean of the individual averages for peak GRF was 3.2 ± 0.2 BW^{-1}. The corresponding stresses were 86 ± 7 kPa. The ratio of LG force (N) to GRF (N) was 0.59 ± 0.07. Despite a relatively strong correlation (r^2=0.88), there was not a significant relationship between LG stress and GRF (p=0.06).

Supplemental Information: Aquatic and terrestrial takeoffs require different hindlimb kinematics and muscle function in mallard ducks
K.R. Taylor-Burt & A.A. Biewener

Supplemental Table 1. Animal information & experimental use

	Sex	Origin	Body Mass (kg)	LG Mass (g)	LG PCSA (cm^2)	Light Kinematics	X-ray Kinematics	Fascicle Length	LG Force	Pennation Angle	EMG
1	F	Wild	0.868			T(3), A(3)					
2	F	Wild	0.841	3.75	1.76	T(3), A(3)		T(2), A(3)		T(2), A(3)	T(2)
3	M	Wild	1.03				T(2), A(2)				
4	M	Wild	1.005	5.01	2.48	T(3), A(3)	T(2), A(2)	T(3)	T(3)*	T(3)	T(3)
5	F	Wild	0.984	4.24	1.57			T(3), A(3)	T(2), A(3)	T(2), A(3)	T(1)
6	M	Farm	0.843			T(3), A(3)	T(2), A(2)				
7	F	Wild	0.712	2.72	1.05			T(2), A(2)			T(2)
8	F	Wild	0.88	4.32	1.89	T(3), A(3)		T(2)	T(3)	T(2)	
9	M	Farm	0.834	4.01	1.68			T(3), A(3)	T(3), A(3)	T(1), A(2)	T(3), A(3)
10	F	Farm	1.008	6.45	2.86			A(3)	A(3)	A(2)	A(3)
11	F	Farm	0.996	5.86	2.72				T(3), A(2)		
12	M	Wild	1.137	4.37	1.67			T(3), A(3)		T(3), A(3)	

T = terrestrial takeoff, A = aquatic takeoff
Numbers in parentheses indicate the number of trials.
* Timing only